

Possible origins of the magnetoresistance gain in colossal magnetoresistive oxide $\text{La}_{0.69}\text{Ca}_{0.31}\text{MnO}_3$: Structure fluctuation and pinning effect on magnetic domain walls

X. Z. Yu,^{1,a)} Run-Wei Li,² T. Asaka,³ K. Ishizuka,¹ K. Kimoto,¹ and Y. Matsui¹

¹Advanced Electron Microscopy Group and High Voltage Electron Microscopy Station, National Institute for Materials Science (NIMS), 1-1 Namiki, Tsukuba 305-0044, Japan

²Ningbo Institute of Materials Technology and Engineering (NIMTE), Chinese Academy of Sciences (CAS), Ningbo, Zhejiang 315201, People's Republic of China

³Japan Fine Ceramics Center (JFCC), 2-4-1 Mutsuno, Atsuta-ku, Nagoya 456-8587, Japan

(Received 31 July 2009; accepted 11 August 2009; published online 2 September 2009)

The spatial fluctuation of the magnetic domain (MD) and charge/orbital ordering (CO/OO) structure at around the Curie temperature (T_C) was directly observed in a colossal magnetoresistance (CMR) compound, $\text{La}_{0.69}\text{Ca}_{0.31}\text{MnO}_3$, in which extraordinary anisotropic magnetoresistance (AMR) has also been observed. It was found that the long range MD structure collapses upon the emergence of short range CO/OO in a narrow temperature regime, which provides abundant evidence in support of a gain in magnetoresistance at around T_C . Moreover, the pinning effect on the MD wall was discerned and it may contribute to the CMR as well as to the extraordinary AMR effect. © 2009 American Institute of Physics. [DOI: 10.1063/1.3216589]

The colossal magnetoresistance (CMR) effect is observed in carrier-doped manganites.¹ It has been pointed out in conjunction with the competition between ferromagnetic (FM) and charge/orbital ordering (CO/OO) structures at around the Curie temperature (T_C).²⁻⁴ FM and CO/OO, as typical phenomena in manganites, are responsible for the double exchange interaction⁵ and the ordering of $\text{Mn}^{3+}/\text{Mn}^{4+}$ in a 1/1 proportion accompanied by e_g -orbital ordering ($3x^2-r^2/3y^2-r^2$ -type CO/OO),^{1,6} respectively. As the FM phase competes with the CO/OO phase, a subtle nanoscale structure fluctuation,^{7,8} and hence the coexistence of the multielectronic phases⁸⁻¹⁰ was observed. On the other hand, the competition between FM and CO/OO triggers drastic changes in electronic structure at around T_C even with weak external stimuli, resulting in peculiar electric and magnetic properties.^{11,12} It is, therefore, desirable to investigate the electronic structure on a nanometer space as well as its variation with temperature and external magnetic field near T_C .

Recently, anisotropic magnetoresistance (AMR) quantified as $\text{AMR} \equiv [(\rho_{\parallel} - \rho_{\perp}) / \rho_{\parallel}] \times 100\%$ (ρ_{\parallel} and ρ_{\perp} are the parallel or perpendicular resistivities to a certain crystalline axis with an applied field along current direction) has been discovered in perovskite manganite thin films, owing to extrinsic effects, such as strain induced by substrates.^{13,14} It is very interesting that the AMR effect has also been demonstrated in single crystalline $\text{La}_{0.69}\text{Ca}_{0.31}\text{MnO}_3$, although the anisotropic CMR is neglected in such pseudocubic manganites with a three-dimensional electronic state and a little anisotropic magnetic structure.¹ This AMR effect has been observed to depend on the temperature and crystal orientation, and to attain a peak near T_C .¹⁵⁻¹⁷

In this study, we aim to shed light on the relevance between the CMR (extraordinary AMR) effect and the electronic structure near T_C by means of the transmission electron microscopy (TEM).¹⁸⁻²² The temperature and external magnetic field dependences of the magnetic domain (MD),

as well as the CO/OO structure, have been systematically studied at around T_C . It was found that, in addition to an electronic structure competition, the pinning effect of twin boundaries on MD walls may be another cause of the CMR and AMR.

$\text{La}_{0.69}\text{Ca}_{0.31}\text{MnO}_3$ single crystal was grown by the floating zone technique. Thin samples were prepared by low-temperature argon-ion thinning method.⁸ The external magnetic field along $[-1, -1, 0]$ -axis was applied *in situ*. The crystal structure and MD structure were studied by analyzing the selected-area electron diffraction (SAED) patterns and Lorentz TEM observation, respectively. The quantitative evaluation of the magnetic components in $\{110\}$ was accomplished by combining TEM observation with the transport-of-intensity equation (TIE) method.^{20,21,23,24}

As shown in Fig. 1(a), $\text{La}_{0.69}\text{Ca}_{0.31}\text{MnO}_3$ has an orthorhombically distorted perovskite structure. Such an orthorhombic structure might cause the anisotropic MD structure, though the crystalline anisotropy is very weak, owing to the strong coupling among charge, spin, and orbital (lattice) degrees of freedom in carrier-doped manganites. As shown in Fig. 1(b),¹⁵ the FM transition occurred at 220 K, where an increase in magnetization accompanied by an abrupt decrease in resistivity is observed. The change in the peak of resistivity indicates that the FM transition temperature (T_C) increases with applied magnetic field.

Since a resistivity peak, CMR, and AMR are observed at around the T_C ,¹⁵ we pay more attention to the magnetic structure ascribed to the spontaneous magnetization, and to the CO/OO structure near T_C . Figure 1(c) show the variations in MD walls with temperature in the (001) plane. These Lorentz TEM images indicate that the original 180° domain walls (shown by white arrows) at 195 K become bent at 198 K and partly broken (see MD walls in region A) with more increasing temperature. This means that the stable long range spin ordering structure becomes a fluctuating one as temperature approaches T_C . At the same time, an increase in the number of domain walls and a decrease in the size of MDs

^{a)}Electronic mail: yu.xiuzhen@nims.go.jp.

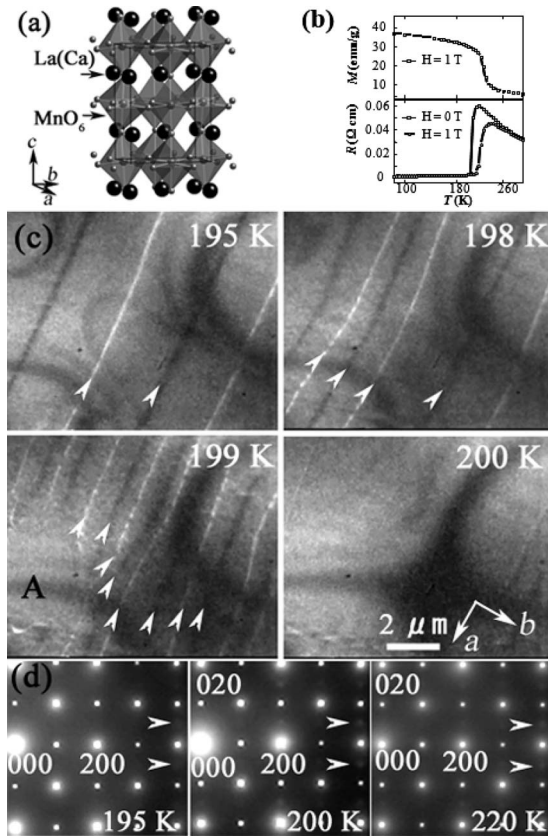


FIG. 1. (a) Schematic of crystal structure. (b) Temperature dependences of magnetization and resistivity. (c) Variation in the MD walls near T_C . White/black lines shown by the white arrows represent the MD walls. (d) [001]-zone SAED patterns at various temperatures. Indexes are based on the orthorhombic setting with the lattice parameters $a_o \sim b_o \sim \sqrt{2}a_p$, and $c_o \sim 2a_p$ (a_p being the lattice parameter of primitive perovskite).

were seen. If the external magnetic field is applied to such a fluctuating MD structure, the magnetoresistance should be induced as a result of spin-dependent scattering at the broken MD walls. It is noted that MDs disappear at 200 K, which is below T_C . The reason is that the transition temperatures obtained by TEM observation and by magnetization measurement are different owing to the increase in T_C with an external magnetic field and also to the use of different temperature measurement systems. Figure 1(d) presents the [001]-zone SAED patterns at 195, 200, and 220 K. In addition to the sharp strong fundamental reflections, broader weak superlattice (SL) reflections (marked by white arrows) are also observed. Such SL reflections indicate the modulation structure with a super unit cell of $a \times 2b \times c$ associated with the $3x^2-r^2/3y^2-r^2$ -type CO/OO structure.²⁵ The SL reflections only appear in a narrow temperature regime (from 195 to 235 K) and peak at 200 K, at which the MDs disappear. The drastic changes in FM and CO/OO structures reveal that the emergence of CO/OO near T_C assists the collapse of the MD structure. This scenario of phase competition may be a possible origin of the magnetoresistance gain and hence of the appearance of a CMR or AMR peak at around T_C .

The three-dimensional MD structure is a key to gaining insight into the magnetic anisotropy and the origin of AMR. Figure 2 shows the Lorentz TEM images of (001) and $\{110\}$ $\text{La}_{0.69}\text{Ca}_{0.31}\text{MnO}_3$ below T_C . The original 180° MD structure in Fig. 2(a) and stripe-shaped MD structure in Figs. 2(b) and 2(c) reveal the uniaxial MD structure with a hard (easy) mag-

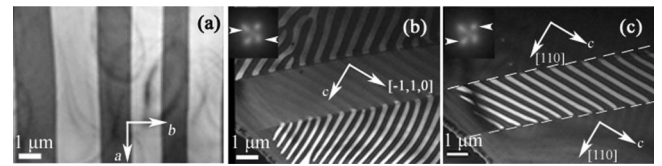


FIG. 2. MD images at a low temperature (~ 195 K): (a) (001) plane, (b) (110) plane, and (c) $(-1,1,0)$ plane. Dashed lines indicate the twin boundaries.

netization direction along the c -(a -) axis. In the twins of (110) and $(-1,1,0)$, the stripe-shaped MDs develop in the single crystalline domain, whereas they locally bend at twin boundaries to form 90° MDs. This 90° MD structure is also demonstrated by the reciprocal space pattern. Insets of Figs. 2(b) and 2(c) show the splitting of a central beam spot into four spots at the diffraction plane (back focal plane) indicating the perpendicular domain structure. One pair of spots [shown by white arrows in Fig. 2(b)] is associated with the antiparallel MDs along the $[110]$ direction, and another pair [shown by white arrows in Fig. 2(c)] corresponds to the antiparallel MDs along the $[-1,1,0]$ direction.

Variations in the MD structure of $\text{La}_{0.69}\text{Ca}_{0.31}\text{MnO}_3$ have also been studied in detail under varying external magnetic fields near T_C , since CMR or AMR occurs under an external magnetic field. Figure 3 demonstrates variants of the MD structure for various magnetic fields along $[-1, -1, 0]$. The reduction of 180° MD walls is observed with a weak magnetic field. As the applied magnetic field exceeds 100 Oe, no domain walls exist within the (001) plane [see Fig. 3(f)], indicating that the magnetization of the (001) thin crystal is saturated. Partially striped MD walls in $\{110\}$ with twins of (110) and $(-1,1,0)$, however, remains around twin boundaries [see Fig. 3(b)] in spite of the formation of a larger MD (see region B) in the single crystal domain. As applied field exceeds 150 Oe, as shown in Fig. 3(c), the extension (contraction) of MDs along $[110]$ $[-1,1,0]$ is driven by the external field. With applied field over 270 Oe, the stripe domains around twin boundaries rarely become a single domain [see Fig. 3(d)]. Changes in the MD structure of (001)

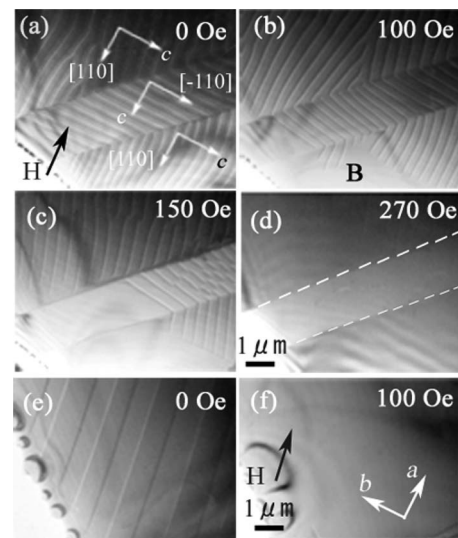


FIG. 3. Changes in MD structures of $\{110\}$ $\text{La}_{0.69}\text{Ca}_{0.31}\text{MnO}_3$ with twins of (110) and $(-1,1,0)$ [(a)-(d)], and of the (001) plane [(e) and (f)] with applied magnetic field along $[110]$ -axis.

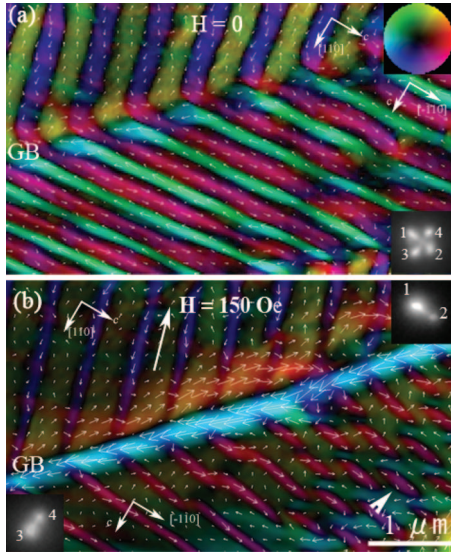


FIG. 4. (Color) Magnetic component distributions in a twin of (110) and $(-1,1,0)$ without external magnetic field (a) and with one of 150 Oe (b). Color wheel shows the magnetization direction in addition to white arrows. The longer arrow indicates the direction of applied magnetic field.

and $\{110\}$ with applied magnetic field show that the formation of a single MD in $\{110\}$ with twins requires a larger magnetic field of three times that required for (001), suggesting that the magnetic components around twin boundaries are only nominally magnetized.

The magnetization distribution map (Fig. 4) of $\{110\}$ with a twin has been determined by the TIE method. As shown in Fig. 4(a), the main parts of the color map of the single crystal domain, such as the blue/green or light blue/pink areas, show that the magnetic components align along $\langle 110 \rangle$ or $\langle -1,1,0 \rangle$ directions, respectively, indicating the 180° MD structure in the single crystal domain and the 90° MD structure at the twin boundary. As we applied an external magnetic field of 150 Oe along the $[-1, -1, 0]$ direction on a twin, the magnetization distribution pattern becomes complex [see Fig. 4(b)]. In (110), the formation of wider (narrower) domains parallel (antiparallel) to the direction of the external field indicates magnetized (demagnetized) effects. Corresponding splitting of the central beam spots is shown in the right upper panel of (b). The two spots with different size and intensity identify the unbalanced-antiparallel MDs as well. In $(-1,1,0)$ perpendicular to the applied field, the tadpole-shaped closure domain (shown by the white arrowhead) has been observed. At the same time, central beam spot splits into a stronger and a weaker spot. A strike line associated with the tadpole-shaped closure domains is observed between the splitting spots. Being analogous to the nucleation of domains around grain boundaries in the longitudinal external field,²⁶ such closure domains arising from the internal transverse domains will resist the 180° MD wall motion. Correspondingly, magnetic components are easily restricted around crystal imperfections, such as twin boundaries. Accordingly, as shown in Fig. 4(b), the local magnetic components mostly align along the twin boundary, indicating that the local magnetic components around a twin boundary are easily pinned. This pinning effect on MD walls,

as well as uniaxial MD structure may be a cause of the AMR effect.

In summary, experimental aspects of magnetic and crystal structures in $\text{La}_{0.69}\text{Ca}_{0.31}\text{MnO}_3$ provide abundant evidence in support of the competition between FM and CO/OO and hence the spatial fluctuation of the spin/charge/orbital ordering structure at around T_C . In addition to the electronic structure competition, the pinning effect of the twin boundaries on MD walls has also been observed at around T_C . Our findings strongly suggest that the pinning effect of twin boundaries in the presence of an external magnetic field, as a manifestation of phase competition, may also contribute to the CMR and extraordinary AMR in pseudocubic perovskite. Controlling the fluctuating structure and crystal orientation may open a way to achieving the expected effect.

We would like to thank Professor Taka-hisa Arima, Dr. Y. Tomioka, Dr. T. Hara, Dr. T. Nagai, Mr. C. Tsuruta, and Ms. W. Z. Zhang for helpful discussions.

- ¹*Colossal Magnetoresistive Oxides*, edited by Y. Tokura (Gordon & Breach, London, 2000).
- ²Y. Tokura and N. Nagaosa, *Science* **288**, 462 (2000).
- ³E. Dagotto, T. Hotta, and A. Moreo, *Phys. Rep.* **344**, 1 (2001).
- ⁴Y. Tokura, *Rep. Prog. Phys.* **69**, 797 (2006).
- ⁵P. W. Anderson and H. Hasegawa, *Phys. Rev.* **100**, 675 (1955).
- ⁶G. C. Milward, M. J. Calderon, and P. B. Littlewood, *Nature (London)* **433**, 607 (2005).
- ⁷X. Z. Yu, R. Mathieu, T. Arima, Y. Kaneko, J. P. He, M. Uchida, T. Asaka, T. Nagai, K. Kimoto, A. Asamitsu, Y. Matsui, and Y. Tokura, *Phys. Rev. B* **75**, 174441 (2007).
- ⁸X. Z. Yu, Y. Tomioka, T. Asaka, K. Kimoto, T. Arima, Y. Tokura, and Y. Matsui, *Appl. Phys. Lett.* **94**, 082509 (2009).
- ⁹E. Dagotto, *Science* **309**, 257 (2005).
- ¹⁰T. Kimura, Y. Tomioka, R. Kumai, Y. Okimoto, and Y. Tokura, *Phys. Rev. Lett.* **83**, 3940 (1999).
- ¹¹Y. Tomioka, A. Asamitsu, H. Kawahara, Y. Moritomo, and T. Y. Tokura, *Phys. Rev. B* **53**, R1689 (1996).
- ¹²H. Kuwahara, Y. Tomioka, A. Asamitsu, Y. Moritomo, and Y. Tokura, *Science* **270**, 961 (1995).
- ¹³J. O'Donnell, J. N. Eckstein, and M. S. Rzchowski, *Appl. Phys. Lett.* **76**, 218 (2000).
- ¹⁴M. Egilmez, R. Petterson, K. H. Chow, and J. Jung, *Appl. Phys. Lett.* **90**, 232506 (2007).
- ¹⁵R.-W. Li, H. Wang, X. Wang, X. Z. Yu, Y. Matsui, Z.-H. Cheng, B.-G. Shen, E. W. Plummer, and J. Zhang, "Anomalous large anisotropic magnetoresistance in a perovskite manganite," *Proc. Natl. Acad. Sci. U.S.A.* (to be published).
- ¹⁶P. G. Radaelli, G. Iannone, M. Marezio, H. Y. Hwang, S. W. Cheong, J. D. Jorgensen, and D. N. Argyriou, *Phys. Rev. B* **56**, 8265 (1997).
- ¹⁷Q. Huang, A. Santoro, J. W. Lynn, R. W. Erwin, J. A. Borchers, J. L. Peng, K. Ghosh, and R. L. Greene, *Phys. Rev. B* **58**, 2684 (1998).
- ¹⁸P. J. Grundy and R. S. Tebble, *Adv. Phys.* **17**, 153 (1968).
- ¹⁹L. Reimer, *Transmission Electron Microscopy* (Springer, Heidelberg, 1997), pp. 264–272.
- ²⁰T. Asaka, X. Z. Yu, Y. Tomioka, Y. Kaneko, T. Nagai, K. Kimoto, K. Ishizuka, Y. Tokura, and Y. Matsui, *Phys. Rev. B* **75**, 184440 (2007).
- ²¹X. Z. Yu, M. Uchida, Y. Onose, J. P. He, Y. Kaneko, T. Asaka, K. Kimoto, Y. Matsui, T. Arima, and Y. Tokura, *J. Magn. Magn. Mater.* **302**, 391 (2006).
- ²²X. Z. Yu, T. Asaka, Y. Tomioka, C. Tsuruta, T. Nagai, K. Kimoto, Y. Kaneko, Y. Tokura, and Y. Matsui, *J. Electron Microsc.* **54**, 61 (2005).
- ²³K. Ishizuka and B. Allman, *J. Electron Microsc.* **54**, 191 (2005).
- ²⁴M. Uchida, Y. Onose, Y. Matsui, and Y. Tokura, *Science* **311**, 359 (2006).
- ²⁵P. Dai, J. A. Fernandez-Baca, N. Wakabayashi, E. W. Plummer, Y. Tomioka, and Y. Tokura, *Phys. Rev. Lett.* **85**, 2553 (2000).
- ²⁶J. B. Goodenough, *Phys. Rev.* **95**, 917 (1954).